Electronic Supplementary Information (ESI)

Intermediate Selectivity in the Oxidation of Phenols using Plasmonic Au/ZnO Photocatalysts

Feng Lin,[a,b,†] Bogdan E. Cojocaru,[c,†] Luke S. Williams,[a,†] Christopher A. Cadigan,[a] Chixia Tian,[a] Maria Nicoleta Grecu,[d] Huolin L. Xin,[e] Shubham Vyas,*[a] Vasile I. Parvulescu,*[c] and Ryan M. Richards*[a]

[a.] *Department of Chemistry, Colorado School of Mines, Golden, CO 80401, USA.*

[b.] *Department of Chemistry, Virginia Tech, Blacksburg, VA 24061.*

[c.] *Department of Organic Chemistry, Biochemistry and Catalysis, University of Bucharest, Bucharest 030016, Romania.*

[d.] *National Institute of Materials Physics, Magurele-Ilfov 077125, Romania.*

[e.] *Center for Functional Nanomaterials, Brookhaven National Laboratory, Upton, NY 11973, USA*

*R.M.R. rrichard@mines.edu;
*V.I.P. vasile.parvulescu@g.unibuc.ro
S.V. svyas@mines.edu

Experimental Section

The preparation selective of flower-like ZnO was described previously (*CrystEngComm* **2013**, *15*, 3780.). In brief, a designated amount of $Zn(NO_3)_2{\cdot}6H_2O$ was dissolved in 200 mL absolute methanol. Then, urea and benzyl alcohol were added to the mixture with a molar ratio of $Zn(NO_3)_2{\cdot}6H_2O$: urea: benzyl alcohol = 1: 0.5: 2. The solution was stirred for 1 h and transferred to an autoclave (Parr Reactor, model #4520). The reaction mixture was purged with Ar for 1 min and then a pressure of 9 bar Ar was imposed before initiating the heating process. The mixture was heated to 200 °C for 5 h, then to 265 °C and maintained for 1.5 h; finally, the vapor inside was vented (i.e., pseudo-supercritical drying). After pseudo-supercritical fluid drying, a powder was collected and subsequently calcined at 500 °C for 6h. The calcination process was performed on a Thermo Scientific ELED BF51866A-1 Lindberg/Blue M moldatherm box furnace with integrated single-program/multi-segment programmable digital controller with over-temperature protection. To synthesize Au/ZnO, ZnO was dispersed in 200 mL of 6 mM trisodium citrate aqueous solution and stirred vigorously for 1 hour. Then, 50 mL of 3 mM $HAuCl_4$ aqueous solution was added to the ZnO solution dropwise and the mixture allowed for reaction overnight under vigorous magnetic stirring. Finally, the product was centrifuged and cleaned with DI water several times and dried at 100 °C for 24 hours. The preparation of Ag/TiO_2 Pt/ZnO and Ag/ZnO was performed under similar conditions. $Cu(NO_3)_2$ was added to the ZnO precursor solution and Cu/ZnO was prepared *in situ* in one pot.

X-ray Diffraction (XRD) was performed on a Philips X-ray diffractometer Model PW1729 operated at 45 kV and 40 mA using Cu Kα radiation. Scanning electron microscopic (SEM) was performed on a JEOL JSM-7000F with a Thermal Scientific Inc. EDS detector. DR-UV-Vis measurements were performed on an Analytic Jena Specord 250 spectrophotometer. UV-Vis absorptance was calculated by subtracting the reflectance from 100% incident light. TEM work was performed on an image corrected FEI Titan operated at 300 kV. EPR measurements were performed at variable temperature (100-360 K) on the compact automatically controlled ADANI CMS 8400 Spectrometer, in X-band (9.1-9.5 GHz) with a 100 KHz modulation. XPS spectra were recorded at room temperature using an SSX-100 spectrometer, Model 206 from Surface Science Instrument. The pressure in the analysis chamber during the analysis was 1.33 mPa. Monochromatized Al–Ka radiation (hυ = 1486.6 eV) was used. It was generated by bombarding the Al anode with an electron gun operated with a beam current of 12mA and acceleration voltage of 10 kV. The spectrometer energy scale was calibrated using the Au $4f_{7/2}$ peak centered at 83.98 eV. Charge correction was made with the C 1s signal of adventitious carbon (C–C or C–H bonds) located at 284.8 eV. An estimated error of ± 0.1 eV can be assumed for all measurements.

Pulse chemisorption was performed by an AutoChemII 2920 station from Micromeritics. The catalyst samples (100 mg), placed in a U-shaped quartz reactor with an inner diameter of 0.5 cm, were pretreated under He at 100 °C for 1 h. Then, the sample was cooled down to RT under a helium flow of 50 ml min^{-1}. Pulses of catechol, hydroquinone and resorcinol (a flow of He saturated with vapours of the probe molecules) were sent to the sample, until surface saturation was reached. The amount of adsorbed molecules was obtained by using a calibration curve.

In a typical phenol oxidation experiment, 15 mg of photocatalyst was added to a 10 mL aqueous solution of 40-ppm phenol. Two UV lamps (purchased from *Vilber Lourmat*, see **Figure S4** for wavelength distribution) centered respectively at 365 nm (VL-340.BL, 413 μW/cm^2) and 254 nm (VL-340.G, 219 μW/cm^2) were used as UV light sources for reactions under UV irradiation, and one visible lamp (150 W Philips Master ColourCDM-T 150W/830, 119 μW/cm^2) was used as visible light source for reactions under visible light irradiation {(UV lamps 120W *2 * 48Lm/W = 11520 Lm versus Vis lamp 150W * 90Lm/W=13500 Lm)}, to irradiate the mixture solution and 30 μL of solution was collected at 30 min intervals for high performance liquid chromatography (HPCL, Agilent Technologies 1260 Infinity with DAD detector. Column Eurosphere C18, flow rate 1 mL/min, CAN: H_2O = 40: 60, λ = 274.5 nm, V_{inj} = 10 μL) analysis. MS analysis (Thermo Scientific VG PROLAB Benchtop QMS) in the range m/z from 2 to 44 was also used to monitor the resulting gaseous products. In order to detect the active species generated in the photocatalytic system, *tert*-butyl alcohol (*t*-BuOH, 10 mmol·L^{-1}) and $AgNO_3$ (6 mmol·L^{-1}) were introduced as ·OH and e^- scavengers, respectively. It was from this analysis that the relative conversions of the six oxidative products were established. The selectivities of these products were then calculated for each of the six products from their individual conversion percentage divided by the total conversion from phenol.

The photoreactors are fitted with cooling fans and, therefore the reactions were performed at room temperature (or slightly above). Tests in dark at room temperature showed negligible conversion of phenol.

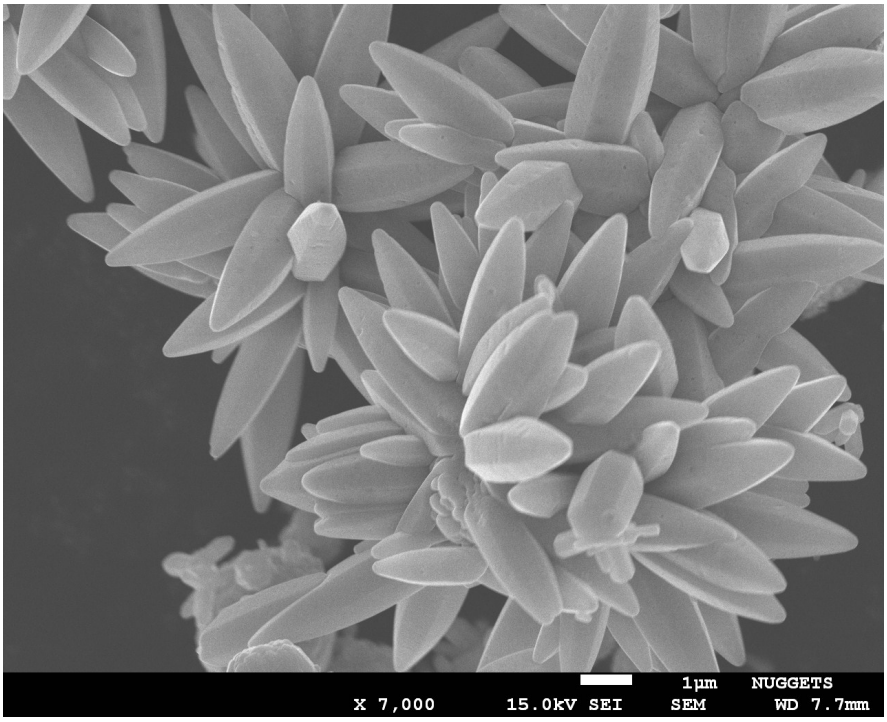

Fig. S1 SEM micrograph of ZnO before Au deposition.

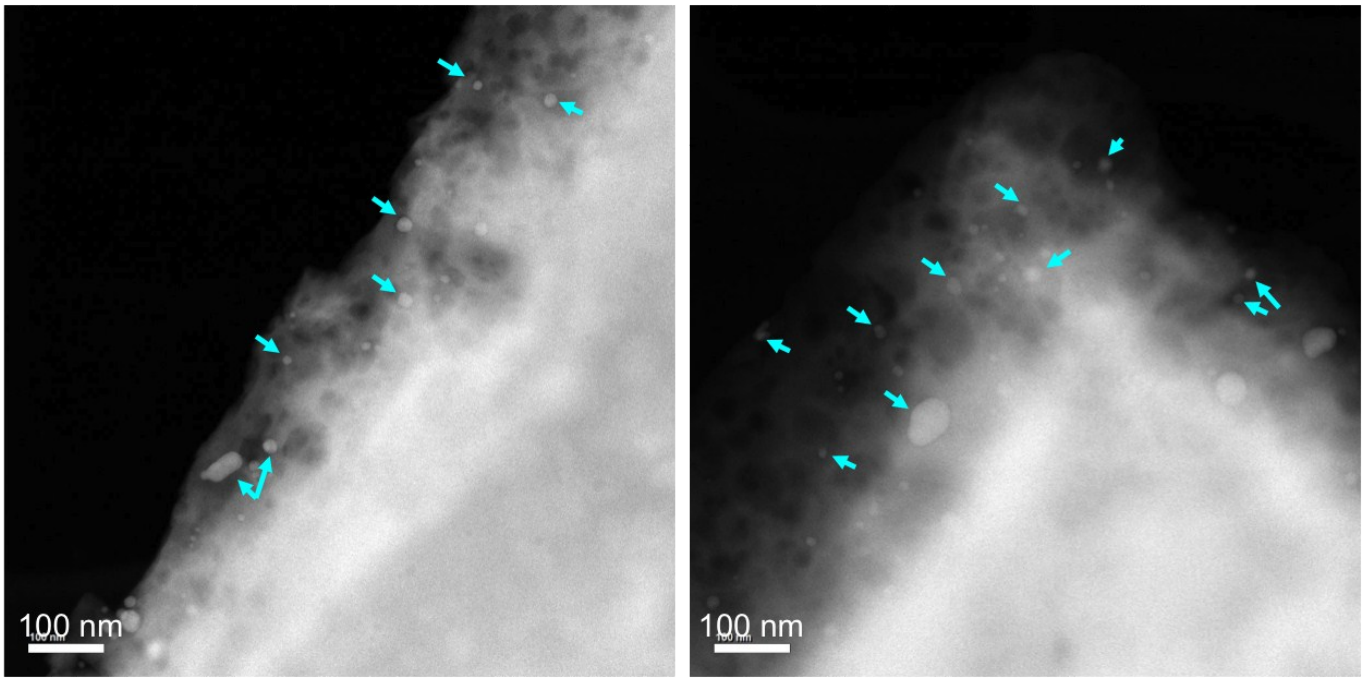

Fig. S2 ADF-STEM images of Au/ZnO composite, where cyan arrows indicate Au nanoparticles. ZnO shows rough surfaces.

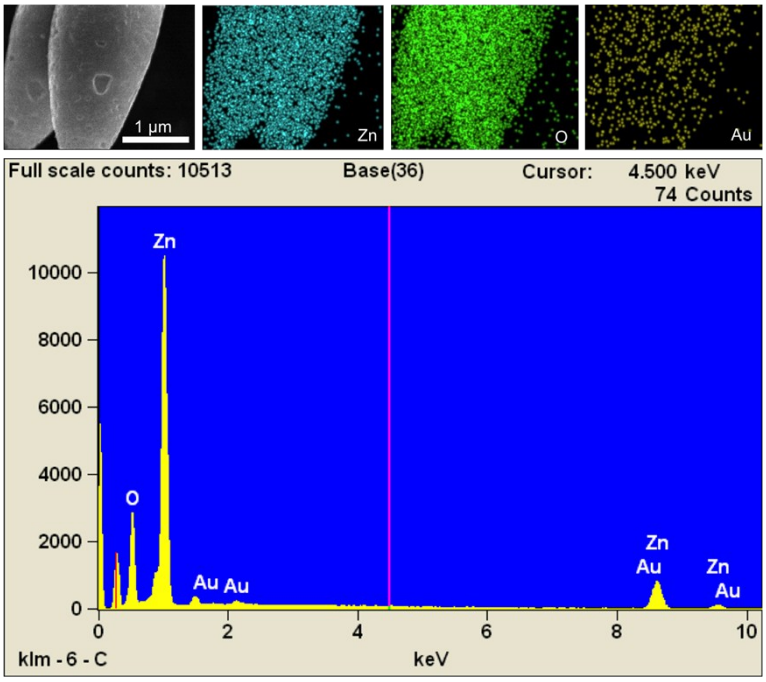

Fig. S3 EDS mapping of the Au/ZnO plasmonic photocatalyst. Quantitative analysis shows that the atomic percentage of Au is 0.3±0.06%.

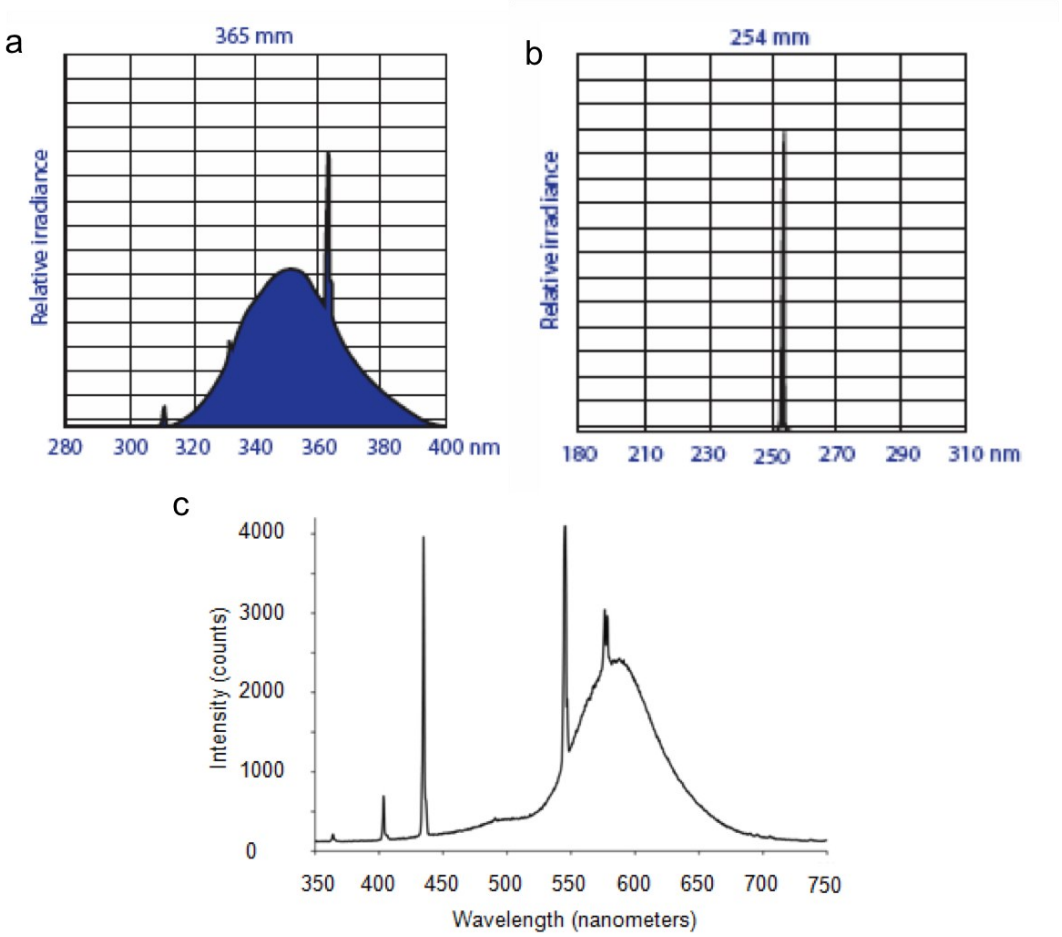

Fig. S4 UV irradiation is composed of (a) and (b), and visible light irradiation is shown in (c).

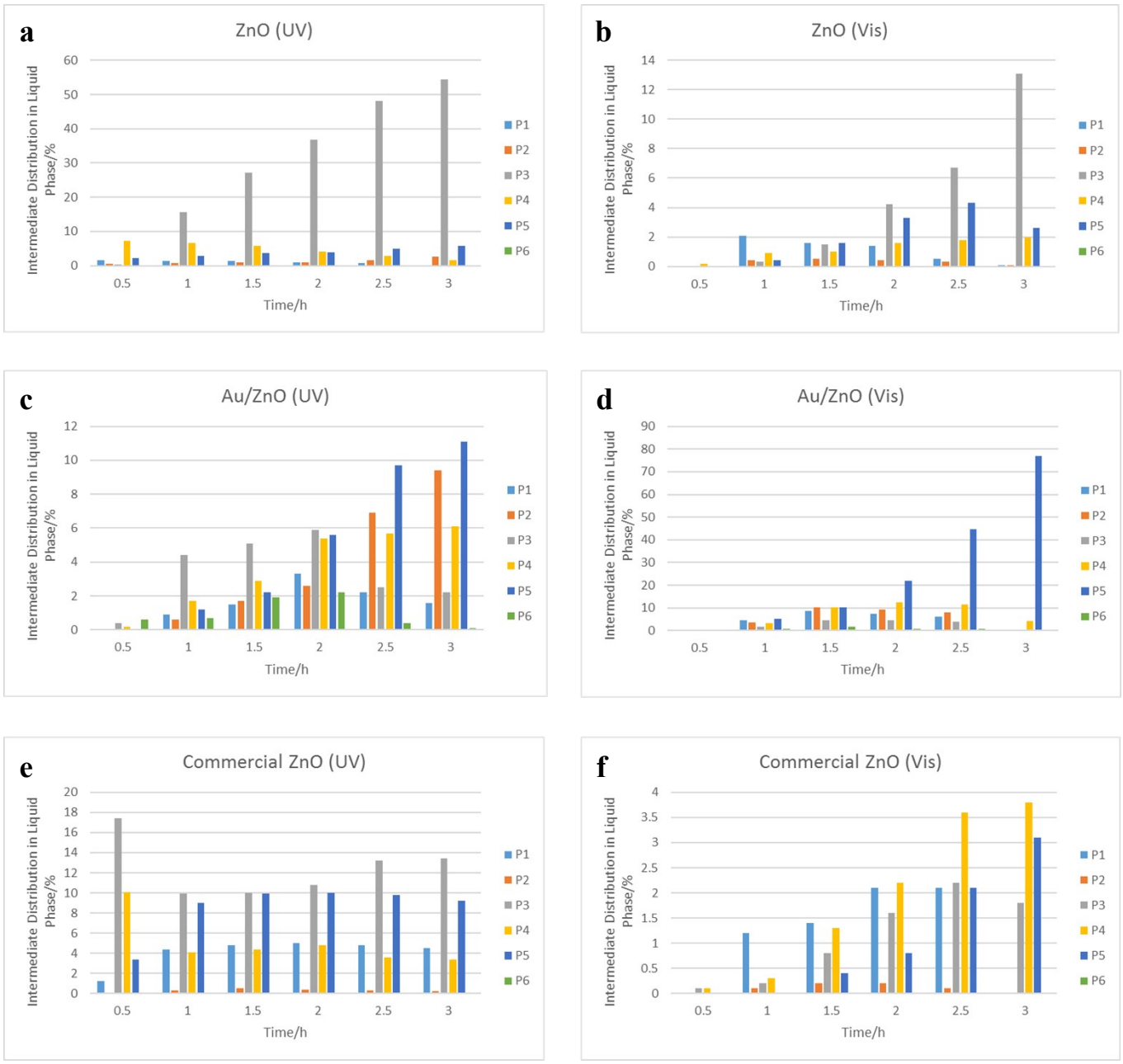

Fig. S5 Graphs of the time-dependent yield for all of the intermediates under control of the various photocatalytic systems. Notice the significant overall conversions for ZnO under UV irradiation and Au/ZnO under visible light irradiation. These constitute the most selective and highest yields of all the trials.

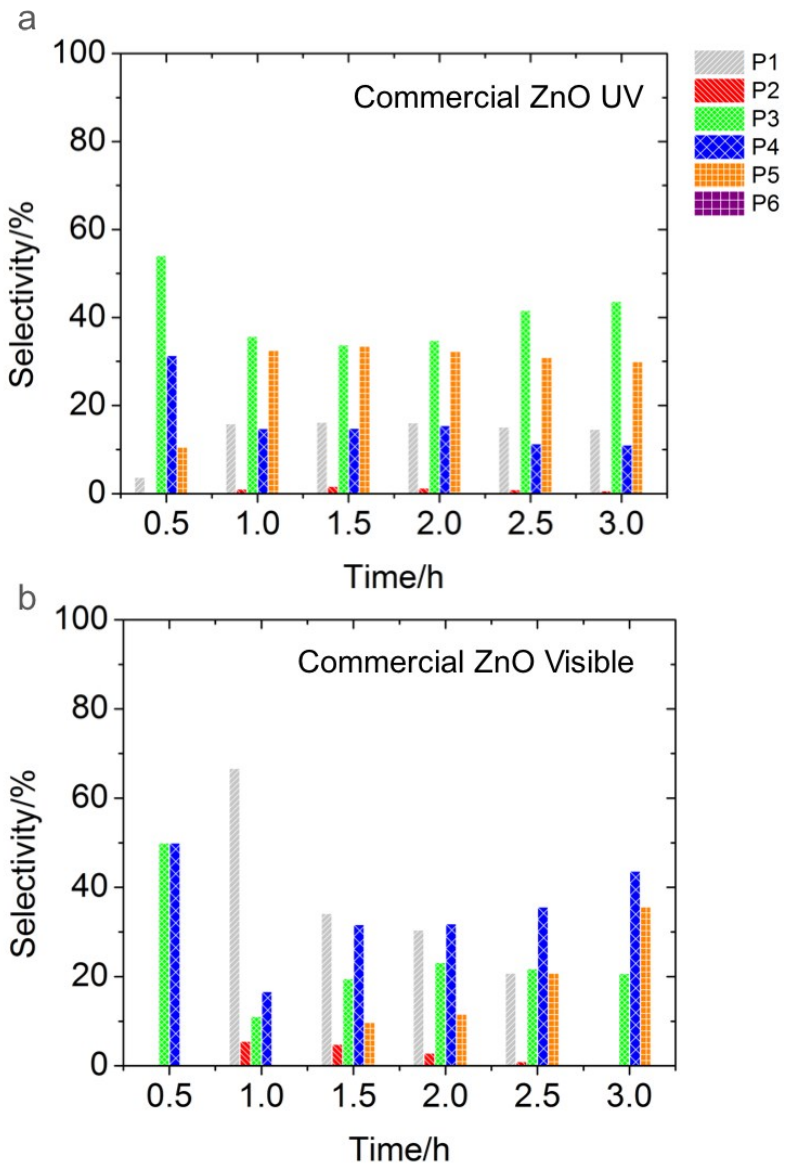

Fig. S6 Time-dependent intermediate selectivity with commercial ZnO: (a) under UV irradiation and (b) under visible irradiation, where P1, P2, P3, P4, P5 and P6 are catechol, 1,2-benzoquinone, resorcinol, hydroquinone, 1,4-benzoquinone and hydroxyquinone, respectively.

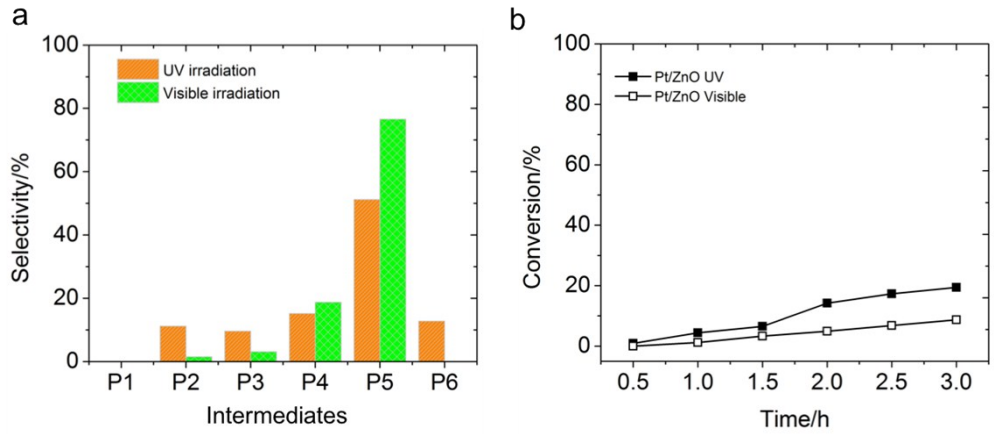

Fig. S7 In the reaction catalyzed by Pt/ZnO: (a) intermediate selectivity of phenol oxidation and (b) time-dependent total conversion of phenol under UV (solid data points) and visible light irradiation (open data points).

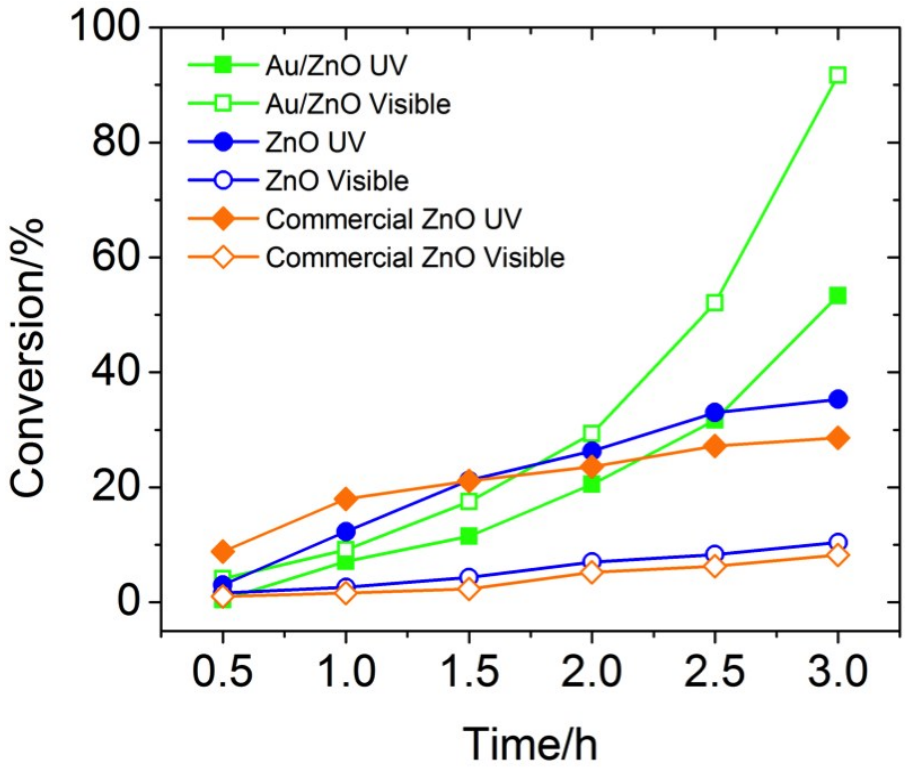

Fig. S8 Time-dependent total conversion of phenol under UV (solid data points) and visible light irradiation (open data points). Au/ZnO shows the best conversion after 3 hours and it delivers higher conversion under visible light irradiation, which is in contrast to the photocatalysts without Au nanoparticles (ZnO and commercial ZnO in the figure), where the conversion is higher under UV irradiation. Major performance variation was found under visible light irradiation, since only under visible light irradiation the Au nanoparticles are excited. The average particle size of Au nanoparticles was 15 nm.

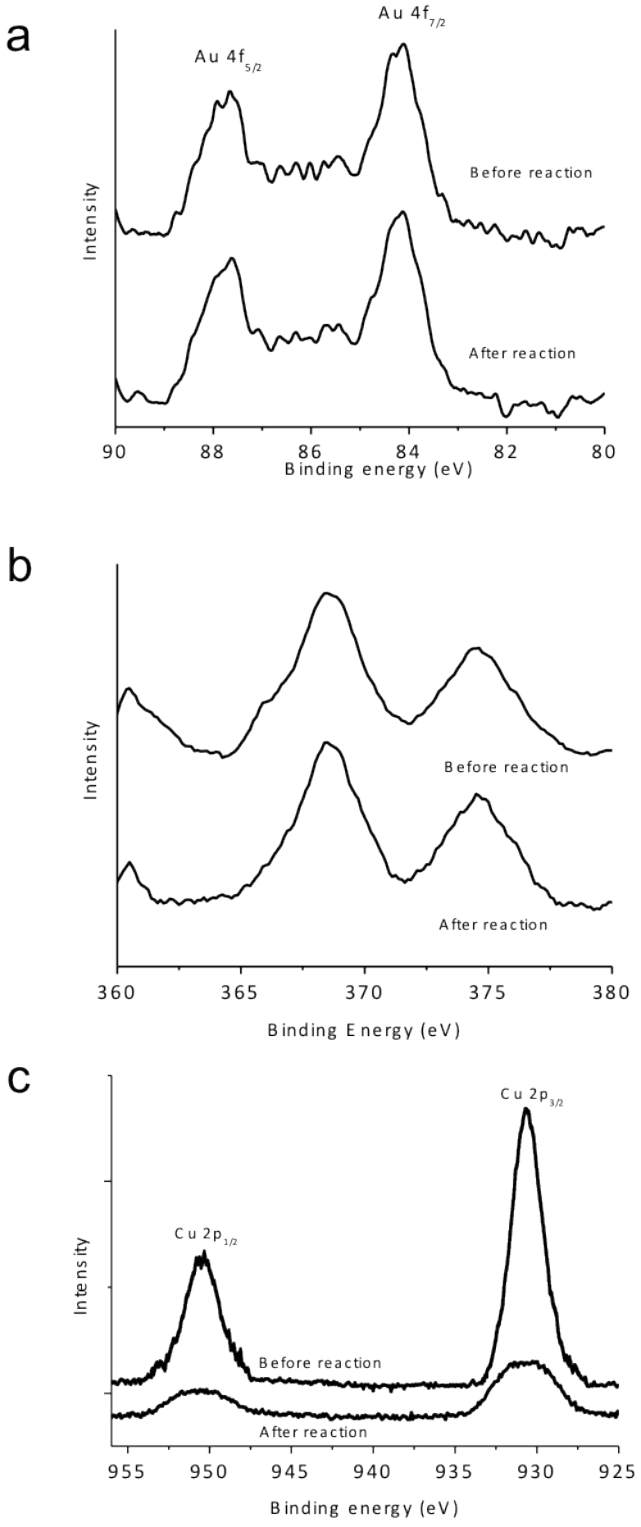

Fig. S9 XPS spectra before and after reaction: (a) Au 4f, (b) Ag 3d and (c) Cu 2p in Au/ZnO, Ag/ZnO and Cu/ZnO, respectively.

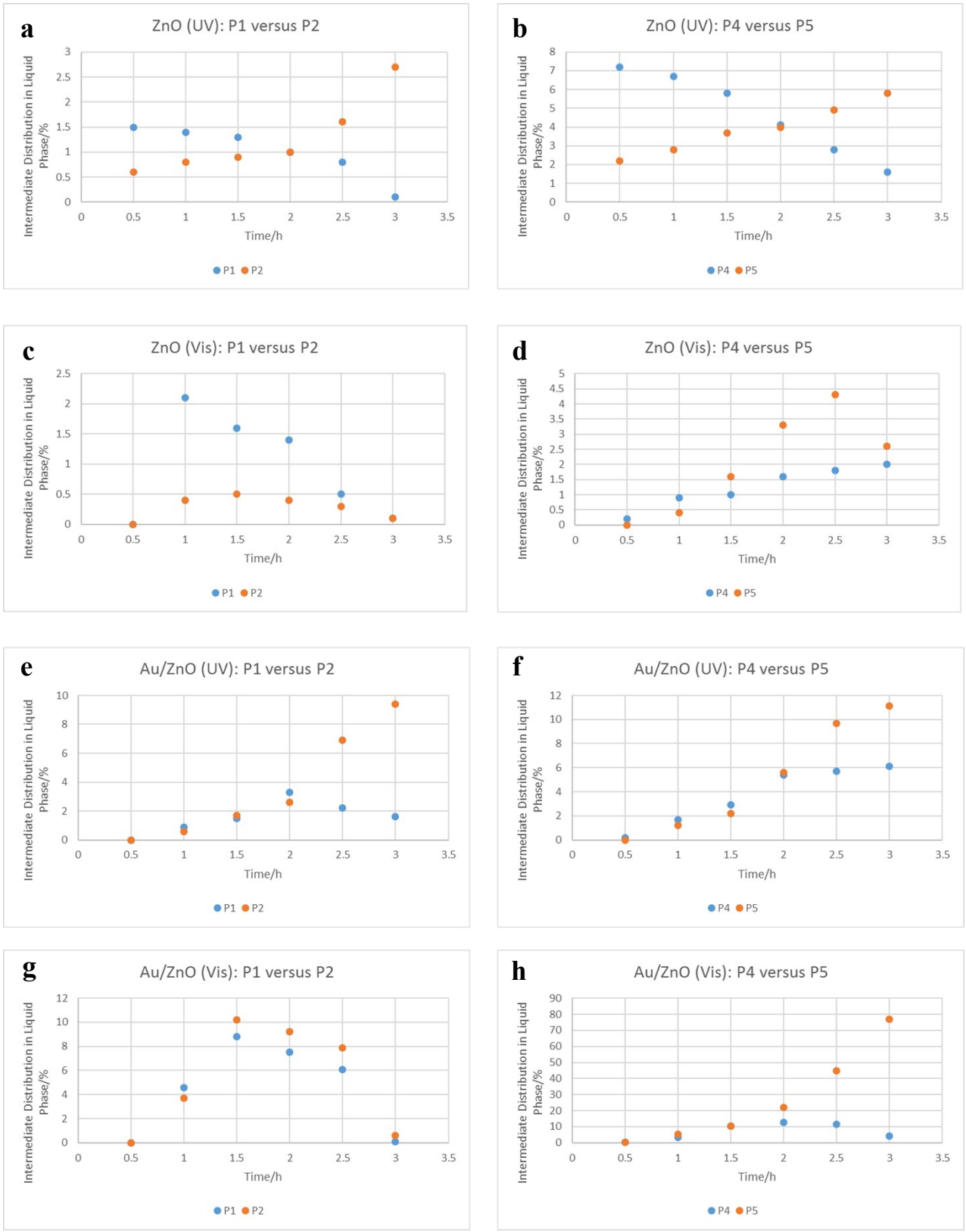

Fig. S10 Inter-conversion of related intermediates: Catechol (P1) conversion to 1,2-benzoquinone (P2) and hydroquinone (P4) conversion to 1,4-benzoquinone (P6) under (a,b) ZnO with UV, (c,d) ZnO with visible light, (e,f) Au/ZnO under UV, and (g,h) Au/ZnO under visible light.

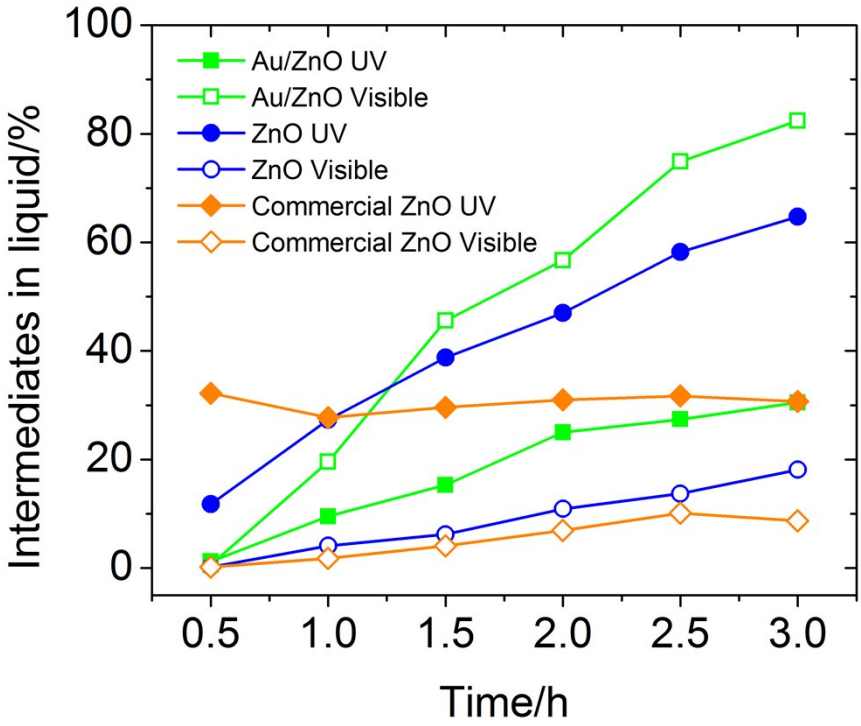

Fig. S11 Time-dependent intermediate percentage in the reaction solution during phenol oxidation under UV (solid data points) and visible light irradiation (open data points).

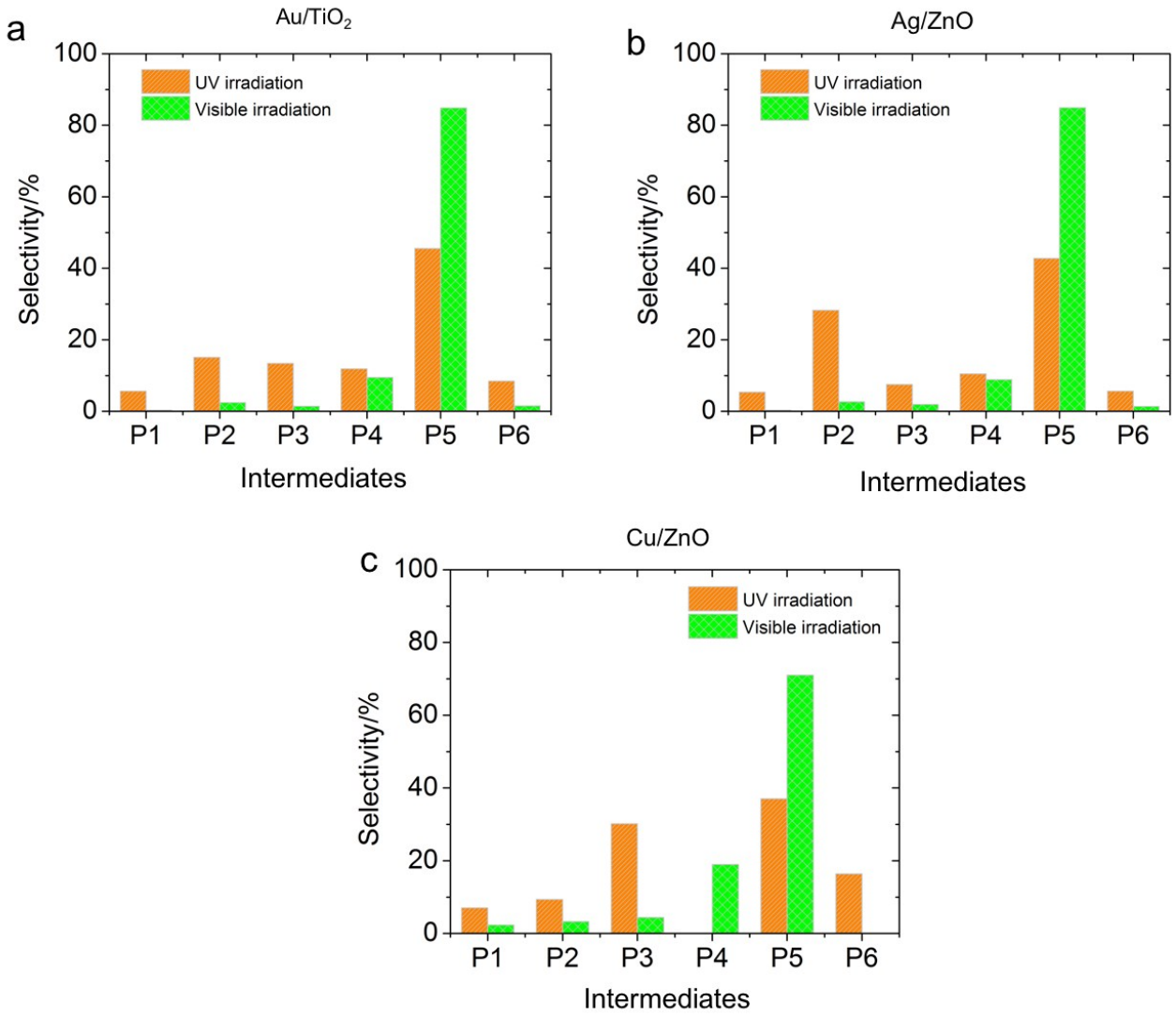

Fig. S12 Intermediate selectivity of phenol oxidation catalyzed by (a) Au/TiO_2, (b) Ag/ZnO and (c) Cu/ZnO, where the intermediates P1, P2, P3, P4, P5 and P6 represent catechol, 1,2-benzoquinone, resorcinol, hydroquinone, 1,4-benzoquinone and hydroxyquinone, respectively. The orange and green columns represent the reactions under UV and visible irradiations, respectively.

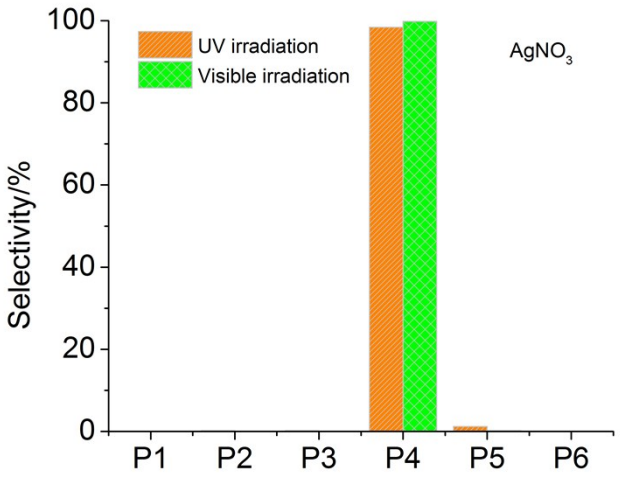

Fig. S13 Intermediate selectivity of phenol oxidation catalyzed by Au/ZnO in presence of $AgNO_3$. Intermediates P1, P2, P3, P4, P5 and P6 represent catechol, 1,2-benzoquinone, resorcinol, hydroquinone, 1,4-benzoquinone and hydroxyquinone, respectively. The orange and green columns represent the reactions under UV and visible irradiations, respectively.

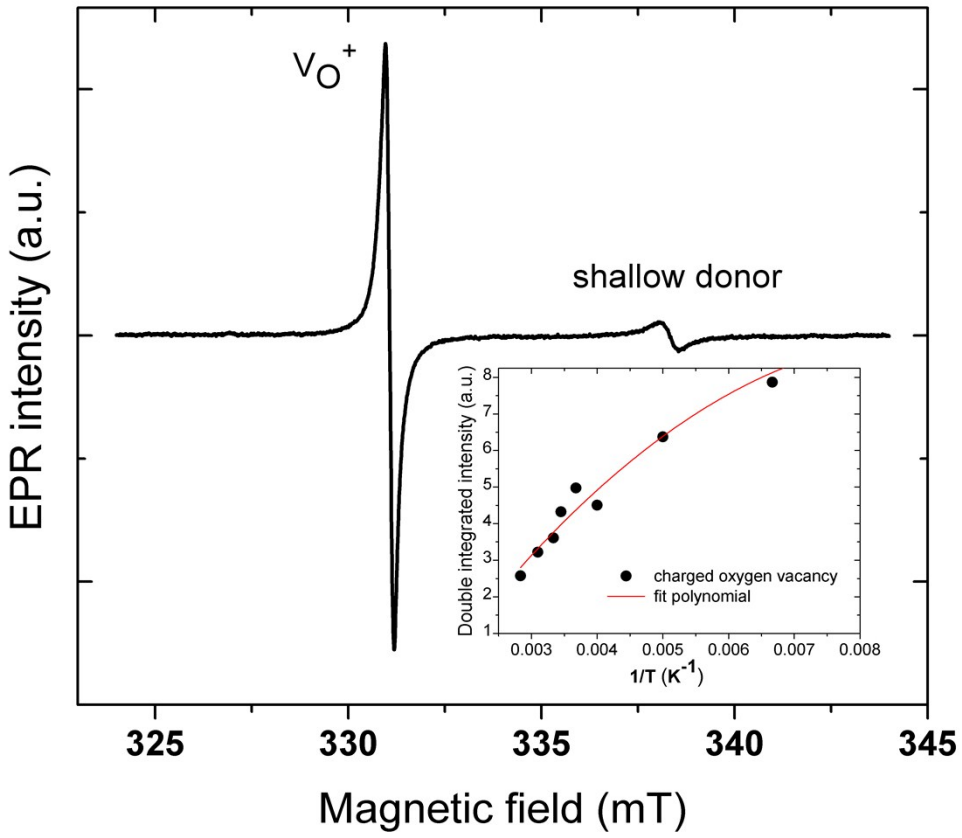

Fig. S14 Room temperature EPR spectrum for ZnO sample; 1/T dependence of single charged oxygen vacancy V_O^+ is shown in the inset.

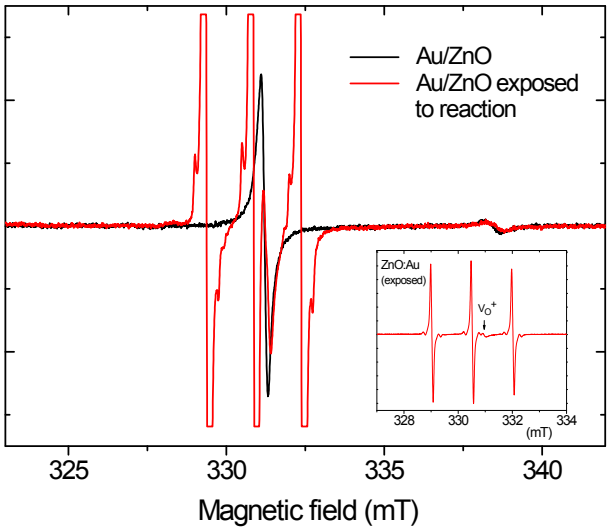

Fig. S15 EPR spectra of Au/ZnO sample as prepared and a 10 mL aqueous solution of 40-ppm phenol, exposed to visible irradiation in N_2 gas at 100 K. The inset shows the ten times reduced spectrum intensity of Au/ZnO exposed.

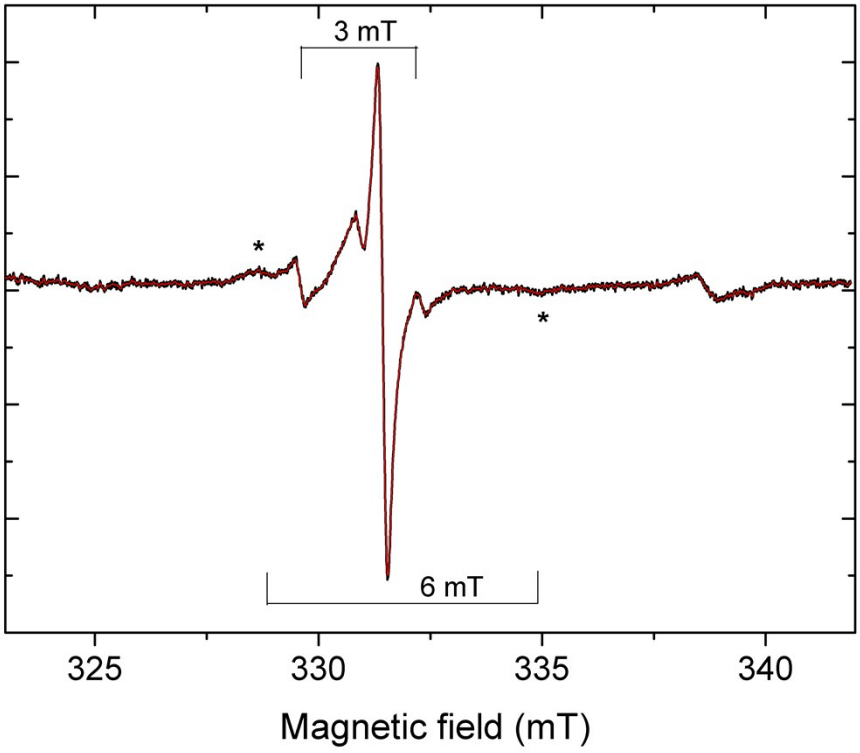

Fig. S16 Room temperature EPR spectra of a 10 mL aqueous solution of 40-ppm phenol, exposed to visible irradiation and exposed at low temperature to N_2 gas, after three weeks; (*) marks the rigid motion regime spectrum.

Electron paramagnetic resonance (EPR) was used to add valuable information regarding the presence of unpaired electrons, such as defects, impurities, and free radicals in ZnO, due to its high sensitivity (being able to reveal 10^{12} spins cm^{-2}). The samples presented here are: ZnO (as prepared), Au/ZnO and Au/ZnO in a 10 mL aqueous solution of 40-ppm phenol, exposed to visible irradiation in N_2 gas at 100 K. These were dried at room temperature (RT) in the ambient atmosphere.

Samples ZnO and Au/ZnO have similar EPR spectrum, of two lines with different intensities, as shown in Fig. S14. Their *g* values are: g_{iso} = 1.997 attributed to singly charged oxygen vacancy (V_O^+) centers; g_{iso} = 1.954 (RT) and axial $g_{//}$ = 1.955 and $g_{\perp}$ = 1.953 (130 K) assigned to intrinsic shallow donor centers. A hyperfine interaction was not observed, thus direct information on the chemical nature of the donors cannot be given.

The sample Au/ZnO in a 10 mL aqueous solution of 40-ppm phenol, exposed to visible irradiation in N_2 gas at 100 K shows an unexpected and very strong EPR signal around g = 2.000+-0.001 (5) at RT, shown in Fig. S15. The well-resolved three line hyperfine structure is due to the unpaired electron interaction with a ^{14}N nucleus (I=1). This signal is attributed to a free radical in a moderate motion regime (the intensity ratio of these three lines is 0.97:1:0.88), which contain the fragment

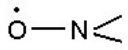

Using the known theory given for such cases [J.H. Freed: J. Chem. Phys. 41, 2077 (1964)] one can estimate the correlation time for molecular motion of the value $\tau_c \sim 2.10^{-9}$ sec. On the other hand, the intensity of V_O^+ center is substantially decreased, while that of the shallow donor is unchanged. By exposing the sample to air for a longer time, a decrease of the new radical intensity is observed, together with the appearance of two additional lines corresponding to the rigid motion regime spectrum (Figure S16).

Computational Section

Thermodynamic and kinetic data was derived from the quantum mechanical treatment of phenol and the six measured products through a series of hydroxyl radical attacks, as shown in **Figure S17.** The rendered scheme shows each intermediate product, with the products of interest labeled. The thermodynamic values (listed alongside each reaction) were calculated as:

$$\Delta H^{\circ}_{rxn} = \sum \Delta H^{f}_{prod} - \sum \Delta H^{f}_{react}$$

Where ΔH^f is taken to be the sum of the electronic and thermal enthalpies of the geometry optimized ground states of the respective molecules. By this convention, negative reaction enthalpies represent exothermic reactions. The rate constants for the principle reaction were generated from optimized transition states. From conventional Transition State Theory, the standard form of the Arrhenius equation was used to calculate the rate constants. Here, $\Delta G^{\ddagger}$ was computed as the difference between the sum of the electronic and thermal free energies of the transition state (TS) and the reactant complex ground state. Reactant complex refers to the lowest energy confirmation of the reactants just prior to forming the TS complex. This provides the rate constant for the forward reaction, as given by:

$$k(T) = \frac{k_B T}{h} * \exp\left(\frac{-\Delta G^{\ddagger}}{RT}\right)$$

It should be noted that the computed values of electronic and thermal enthalpy and free were not scaled to take into account zero-point energy corrections.

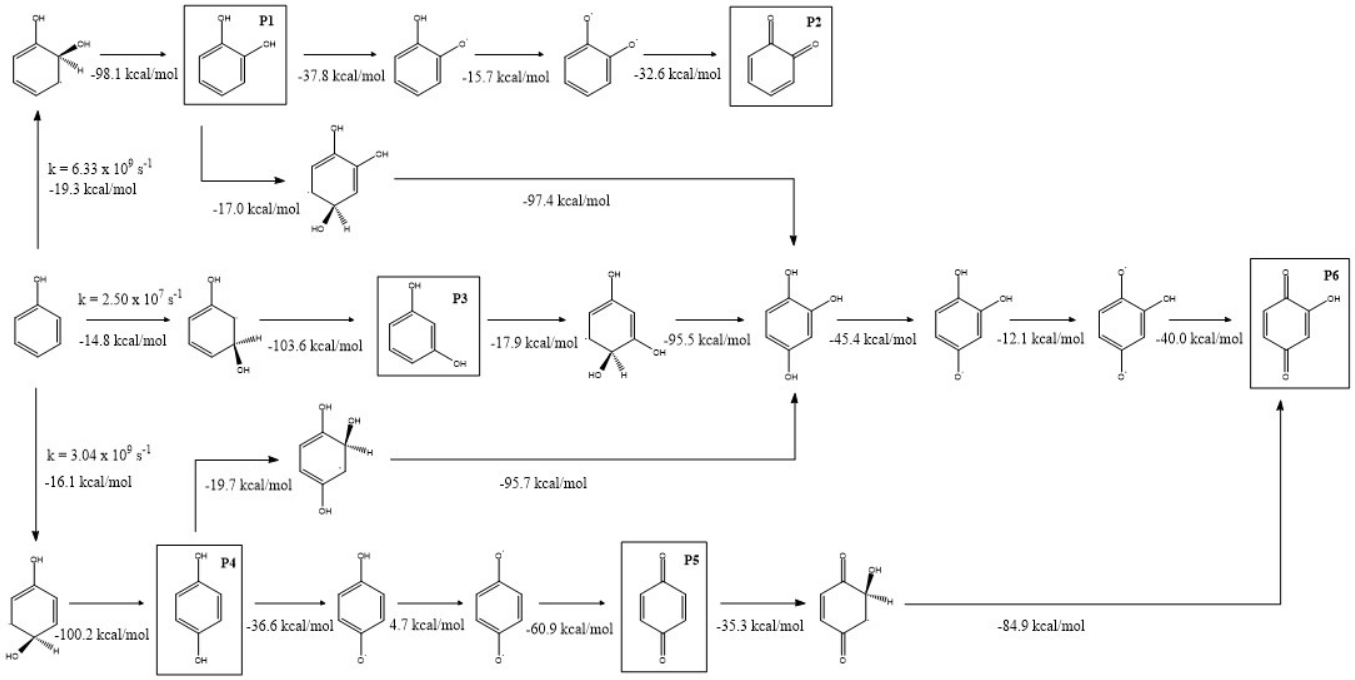

Fig. S17 Chemical scheme illustrating the various reaction pathways taken from phenol to the products of interest (P1-P6) under hydroxyl radical attack. Intermediary structures are included in the step by step reaction process. The values listed in kcal/mol are the reaction enthalpies for each step of the reaction. The second-order rate constant for the primary radical hydroxyl addition to phenol at the *ortho*, *meta*, and *para* positions are also included.

Atom Coordinates for Optimized Ground State Geometries

Phenol

Symbol	x	y	z	Internal Energy (Hartree)
C	-1.848173	0.031653	-0.00007	-307.4434709
C	-1.121876	1.215895	-0.00002	
C	0.267197	1.193323	0.000075	
C	0.933931	-0.027078	0.000032	
C	0.216354	-1.218861	0.000088	
C	-1.170432	-1.183078	0.000045	
H	-2.928277	0.054083	-0.000184	
H	-1.635308	2.167539	-0.000137	
H	0.833445	2.116034	0.000068	
H	0.754496	-2.156474	0.000293	
H	-1.724195	-2.111903	0.000145	
O	2.294817	-0.113573	-0.000359	
H	2.679308	0.76818	0.001785	

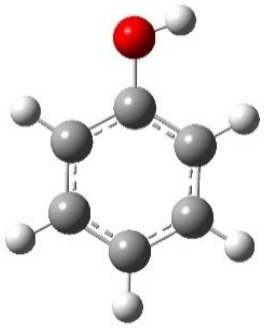

CatecholR

Symbol	X	Y	Z	Internal Energy (Hartree)
C	1.909525	-0.599163	-0.007153	-383.2113503
C	0.805136	-1.350598	0.228313	
C	-0.551295	-0.746082	0.379981	
C	-0.55145	0.728414	0.109199	
C	0.582063	1.452072	-0.111376	
C	1.831135	0.809169	-0.155866	
H	2.874255	-1.081352	-0.09186	
H	0.869611	-2.423922	0.346232	
H	0.499248	2.517503	-0.277321	
H	2.725587	1.383107	-0.344178	
O	-1.761204	1.327971	0.121945	
H	-2.441993	0.643778	0.082162	
O	-1.552966	-1.390591	-0.426495	
H	-1.237696	-1.394708	-1.337438	
H	-0.926343	-0.906309	1.400213	

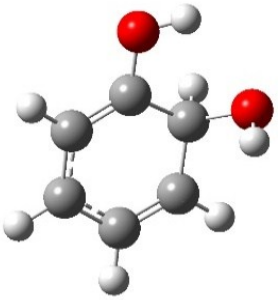

Catechol

Symbol	X	Y	Z	Internal Energy (Hartree)
C	1.870031	0.731072	0.000011	-382.6729551
C	0.647273	1.396529	-0.000001	
C	-0.531747	0.671698	0.000002	
C	-0.498235	-0.724932	0.000009	
C	0.718628	-1.383986	-0.000006	
C	1.904608	-0.655777	-0.000003	
H	2.787257	1.301928	0.000014	
H	0.606439	2.478237	-0.000029	
H	0.722856	-2.465147	-0.000016	
H	2.850671	-1.177662	-0.000015	
O	-1.657081	-1.439567	0.000009	
H	-2.399845	-0.824648	0.000135	

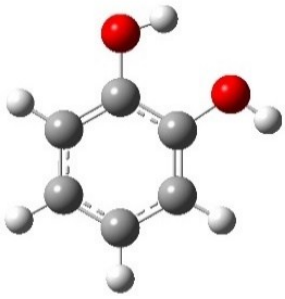

O	-1.78108	1.226244	-0.000086
H	-1.725435	2.186252	0.00045

CatecholR2

Symbol	X	Y	Z	Internal Energy (Hartree)
C	-1.884847	0.597179	0	-382.0361491
C	-0.776036	1.387463	0	
C	0.534342	0.793413	0	
C	0.603717	-0.66585	0	
C	-0.540966	-1.44795	0	
C	-1.770904	-0.818919	0	
H	-2.86989	1.041341	0	
H	-0.838409	2.466476	0	
H	-0.454639	-2.524771	0	
H	-2.670931	-1.416955	0	
O	1.81605	-1.202408	0	
H	2.447423	-0.460844	0	
O	1.608277	1.43025	0	

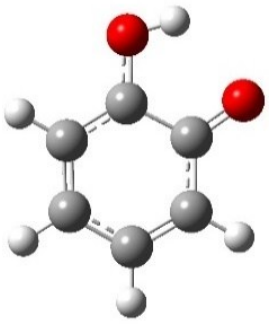

CatecholR3

Symbol	X	Y	Z	Internal Energy (Hartree)
C	-1.832895	-0.67997	0.000001	-381.3627299
C	-0.598875	-1.398183	0.000003	
C	0.67822	-0.749	-0.000001	
C	0.67822	0.749	0.000001	
C	-0.598875	1.398183	-0.000003	
C	-1.832895	0.67997	-0.000001	
H	-2.760346	-1.233063	0.000003	
H	-0.599066	-2.479325	0.000008	
H	-0.599066	2.479325	-0.000008	
H	-2.760346	1.233063	-0.000003	
O	1.735089	1.393791	0.000004	
O	1.735089	-1.393791	-0.000004	

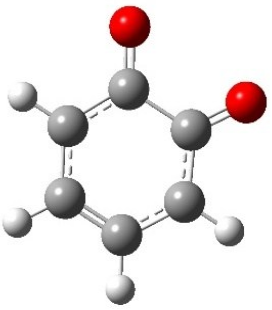

1,2-Benzoquinone

Symbol	X	Y	Z	Internal Energy (Hartree)
C	-0.636909	-1.456072	0.000043	-381.4167166
C	0.665134	-0.778721	-0.000033	
C	0.665135	0.7787	-0.000014	
C	-0.636885	1.455956	-0.000066	
C	-1.762738	0.734279	-0.000022	
C	-1.762753	-0.734345	0.000055	
H	-0.636308	-2.536688	0.000075	
H	-2.7238	1.230114	-0.00004	
H	-0.636351	2.536565	-0.000112	
O	1.720906	1.36348	0.000097	
H	-2.724342	-1.229277	0.000039	
O	1.720956	-1.363418	-0.000066	

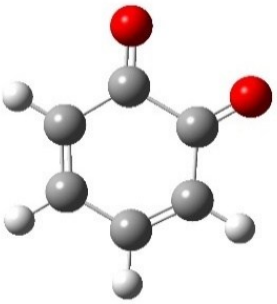

ResorcinolR

Symbol	X	Y	Z	Internal Energy (Hartree)
C	1.235089	-0.413348	0.395721	-383.2034459
C	-0.126877	-1.010496	0.27466	
C	-1.220804	-0.25601	0.019417	
C	-1.13166	1.15221	-0.153123	
C	0.124207	1.782842	-0.060715	
H	2.213911	1.561952	0.264933	
H	-2.030818	1.711528	-0.363689	
H	0.182896	2.853142	-0.204268	
O	-2.48098	-0.771184	-0.095538	
H	-2.455246	-1.724277	0.033468	
H	-0.210873	-2.082969	0.400015	
O	2.090316	-1.075854	-0.558005	
H	3.002515	-0.858682	-0.342129	
H	1.631599	-0.637952	1.39614	

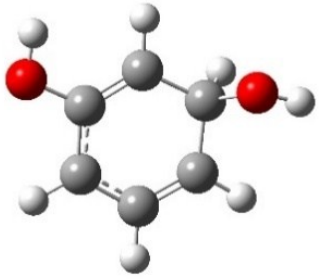

Resorcinol

Symbol	X	Y	Z	Internal Energy (Hartree)
C	-1.224832	1.068202	0.000144	-382.6744143
C	-1.187307	-0.321767	0.000082	
C	0.025778	-1.000963	0.000051	
C	1.210265	-0.276751	-0.00003	
C	1.194835	1.115546	-0.000099	
C	-0.025978	1.771156	0.000026	
H	-2.17338	1.587614	0.000128	
H	2.128851	1.657814	-0.000212	
H	-0.047673	2.852059	-0.000007	
O	2.426382	-0.889883	-0.000137	
H	2.314799	-1.845296	0.001436	
H	0.031547	-2.08287	0.000043	
O	-2.316079	-1.083332	-0.000246	
H	-3.093131	-0.516144	0.000625	

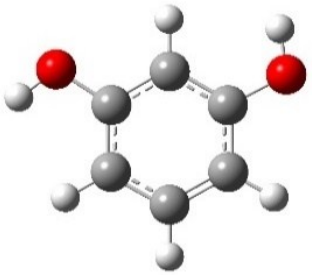

HydroquinoneR

Symbol	X	Y	Z	Internal Energy (Hartree)
C	1.376075	-0.027221	-0.043322	-383.2060642
C	0.660426	-1.241786	0.076485	
C	-0.674586	-1.237192	0.301476	
C	-1.48107	0.023522	0.374722	
C	-0.634181	1.252709	0.302846	
C	0.703666	1.208863	0.085712	
H	1.210155	-2.170354	-0.004316	
H	-1.210131	-2.171734	0.407963	
H	-1.139631	2.202995	0.406265	
H	1.275644	2.126792	0.018954	
O	-2.428184	0.094545	-0.718985	
H	-3.124901	-0.547881	-0.551933	
O	2.710462	-0.109743	-0.262007	

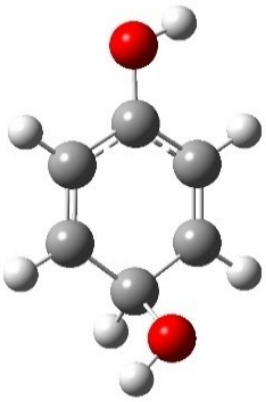

H	3.094619	0.771214	-0.318809
H	-2.065969	0.037182	1.3023

Hydroquinone

Symbol	X	Y	Z	Internal Energy (Hartree)
C	-1.391191	0.027781	0.000004	-382.6710388
C	-0.670807	1.214576	-0.000001	
C	0.716825	1.187217	-0.000002	
C	1.39119	-0.027791	-0.000016	
C	0.670808	-1.214582	-0.000002	
C	-0.716827	-1.187224	0.000019	
H	-1.201984	2.155971	-0.000019	
H	1.274727	2.114772	0.000006	
H	1.201982	-2.155978	-0.000021	
H	-1.274728	-2.114779	0.000046	
O	2.757298	-0.113485	-0.00002	
H	3.139203	0.768804	0.000186	
O	-2.757292	0.1135	0.000003	
H	-3.139238	-0.768764	-0.000074	

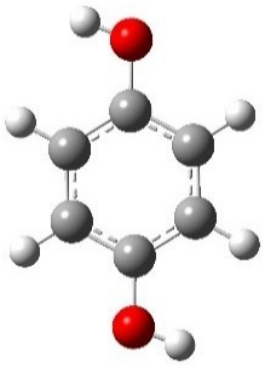

HydroquinoneR2

Symbol	X	Y	Z	Internal Energy (Hartree)
C	1.4913	-0.009675	0	-382.0322206
C	0.719885	-1.234132	0.000001	
C	-0.643381	-1.214053	0.000002	
C	-1.325235	0.019745	0.000001	
C	-0.61624	1.239611	0	
C	0.74529	1.231442	0	
H	1.265216	-2.167462	0.000001	
H	-1.215165	-2.133104	0.000003	
H	-1.180692	2.161461	0	
H	1.311074	2.152609	0.000001	
O	-2.66033	0.095336	0	
H	-3.056841	-0.783492	-0.000019	
O	2.741167	-0.023791	-0.000002	

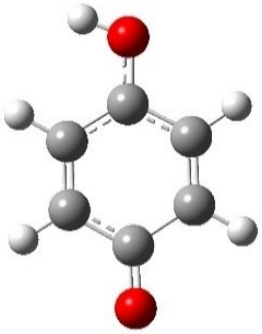

HydroquinoneR3

Symbol	X	Y	Z	Internal Energy (Hartree)
C	-1.453358	0	0.000001	-381.3257235
C	-0.669838	-1.232619	0	
C	0.669838	-1.232619	0	
C	1.453358	0	-0.000001	
C	0.669838	1.232619	0	
C	-0.669838	1.232619	0	
H	-1.24271	-2.148161	0	
H	1.24271	-2.148161	0	
H	1.24271	2.148161	0.000002	
H	-1.24271	2.148161	-0.000002	
O	2.689144	0	0	
O	-2.689144	0	0	

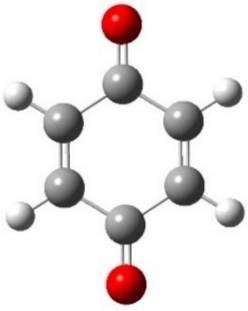

1,4-Benzoquinone

Symbol	X	Y	Z	Internal Energy (Hartree)
C	0.665308	-1.271755	0.000078	
C	-0.665399	-1.27174	0.000094	
C	-1.429738	-0.000007	0.000031	
C	-0.665392	1.271746	0.000087	
C	0.665314	1.271763	0.000086	
C	1.42968	-0.000002	0.000069	
H	1.248971	-2.18232	0.000091	
H	1.248993	2.182319	0.000111	
H	-1.249056	2.182203	0.000135	
O	-2.643043	0.000003	-0.000194	
O	2.643229	-0.000005	-0.000201	
H	-1.249038	-2.182212	0.000155	

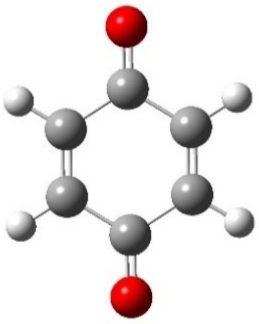

HydroxyquinoneR

Symbol	X	Y	Z	Internal Energy (Hartree)
C	0.572112	-1.165849	0.01302	-457.2191774
C	-0.796786	-0.745058	0.395361	
C	-1.087947	0.703157	0.019494	
C	0.033608	1.65525	0.119584	
C	1.295151	1.220681	0.096333	
C	1.644499	-0.220803	-0.037582	
H	0.776232	-2.212485	-0.161308	
H	2.131304	1.906861	0.115907	
O	-1.768608	-1.619253	-0.099507	
H	-2.570513	-1.09917	-0.241634	
H	-0.215639	2.707335	0.141455	
O	-2.20543	1.023369	-0.311291	
O	2.815859	-0.561561	-0.213515	
H	-0.819776	-0.727247	1.502829	

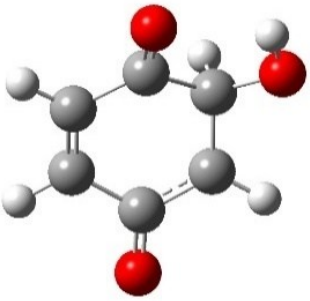

Hydroxyquinone

Symbol	X	Y	Z	Internal Energy (Hartree)
C	0.521461	1.178948	-0.000033	-456.659975
C	-0.755868	0.77265	0.00007	
C	-1.103514	-0.690631	0.000312	
C	0.015097	-1.657621	-0.000058	
C	1.278053	-1.244123	-0.000139	
C	1.615696	0.206027	0.000115	
H	0.792239	2.226522	-0.000245	
H	2.116045	-1.927341	-0.000193	
O	-1.835123	1.55676	-0.000023	
H	-1.579309	2.486492	-0.000457	
H	-0.26289	-2.702428	-0.000106	
O	-2.257825	-1.048	-0.000077	
O	2.781495	0.556897	0.000025	

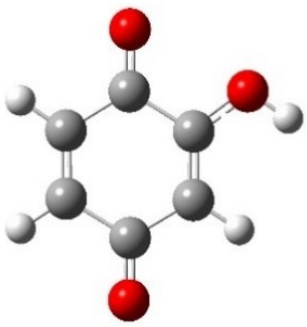

CatecholOHR

Symbol	X	Y	Z	Internal Energy (Hartree)
C	-0.531687	1.145961	0.310243	-458.4371462
C	0.737635	0.744931	0.090043	
C	1.070907	-0.635621	-0.043327	
C	0.065216	-1.612438	0.077797	
C	-1.223543	-1.253542	0.301825	
H	-2.230245	0.339285	1.299643	
H	-0.761002	2.197963	0.420245	
H	0.352545	-2.652277	-0.0037	
H	-1.989515	-2.01043	0.406733	
O	2.348432	-1.010234	-0.262804	
H	2.901647	-0.219982	-0.312794	
O	1.819058	1.573486	-0.010936	
H	1.546094	2.492795	0.063802	
O	-2.561019	0.491255	-0.721295	
H	-3.386601	0.018972	-0.574363	

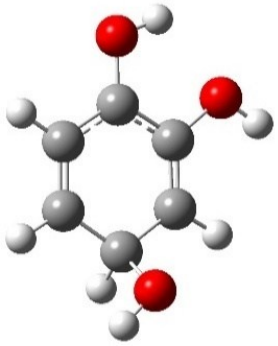

1,2,4-Benzenetriol

Symbol	X	Y	Z	Internal Energy (Hartree)
C	1.587361	0.014255	0.000016	-457.8976961
C	1.154048	-1.30147	-0.000017	
C	-0.210532	-1.57001	-0.000016	
C	-1.142675	-0.546867	0.000019	
C	-0.696965	0.776737	0.000022	
C	0.662631	1.053788	0.000041	
H	1.876654	-2.104066	-0.000067	
H	-0.555679	-2.596274	-0.000059	
H	0.996039	2.084839	0.000044	
O	-2.49552	-0.750851	0.000026	
H	-2.676436	-1.695048	-0.000049	
O	2.935275	0.24222	0.000025	
H	3.111383	1.187228	-0.000268	
O	-1.646125	1.752166	-0.000059	
H	-1.224196	2.616446	0.000075	

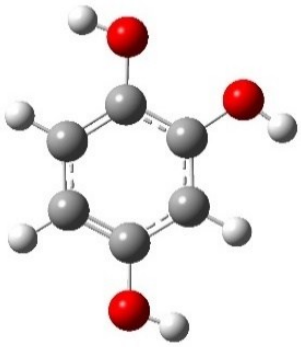

1,2,4-BenzenetriolR2

Symbol	X	Y	Z	Internal Energy (Hartree)
C	-1.535825	-0.097168	0	-457.2729711
C	-1.166407	1.271967	0	
C	0.147511	1.627283	0	
C	1.178688	0.628305	0	
C	0.745952	-0.764404	0	
C	-0.582436	-1.115901	0	
H	-1.955277	2.010288	0	
H	0.45108	2.664613	0	
H	-0.875357	-2.157142	-0.000001	
O	2.408081	0.864168	0	
O	-2.852073	-0.34878	0	

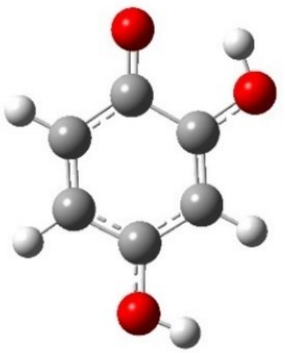

H	-3.024535	-1.296883	-0.000001
O	1.710098	-1.68178	0
H	2.550348	-1.190235	0.000001

1,2,4-BenzenetriolR3

Symbol	X	Y	Z	Internal Energy (Hartree)
C	-1.670488	0.13685	-0.000054	-456.594389
C	-1.226377	-1.244656	-0.00009	
C	0.084123	-1.601711	-0.000054	
C	1.152581	-0.636289	0.000175	
C	0.744361	0.743434	-0.000012	
C	-0.645218	1.143973	0.000357	
H	-2.002117	-1.998125	-0.000184	
H	0.368557	-2.645601	-0.000246	
H	-0.907174	2.192289	0.001272	
O	2.382287	-0.879894	0.00018	
O	-2.873215	0.471325	-0.00012	
O	1.663629	1.660348	-0.000287	
H	2.525238	1.187603	-0.000963	

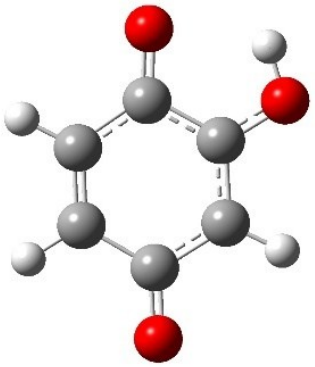

HydroxyquinoneOHR

Symbol	X	Y	Z	Internal Energy (Hartree)
C	-0.332179	-1.540351	0.182019	-458.4398619
C	-1.185033	-0.517446	-0.133989	
C	-0.72699	0.891134	-0.364147	
C	0.761373	1.010322	-0.368753	
H	1.729904	-2.118621	0.493073	
H	-0.732507	-2.527315	0.377149	
H	1.175894	1.983643	-0.598452	
O	-2.520941	-0.658411	-0.251776	
H	-2.779556	-1.570864	-0.081564	
O	2.929285	0.064739	0.004365	
H	3.200646	0.965814	-0.195734	
O	-1.324781	1.776275	0.602794	
H	-0.893917	1.607666	1.447563	
H	-1.149493	1.23906	-1.311701	

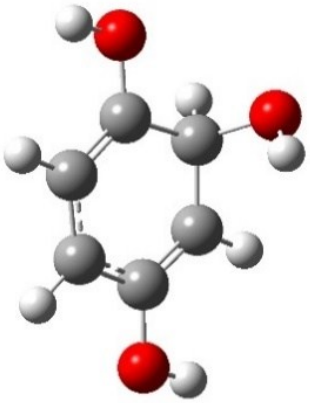

ResorcinolOHR

Symbol	X	Y	Z	Internal Energy (Hartree)
C	-0.565228	1.128364	-0.036127	-458.4400748
C	0.72944	0.782959	0.163497	
C	1.202022	-0.627879	0.326334	
C	0.068733	-1.596123	0.358363	
C	-1.224771	-1.222738	0.157069	
H	-0.852214	2.162505	-0.176907	
H	0.320162	-2.632702	0.531633	
H	-2.01354	-1.965228	0.168103	
O	2.079508	-0.989477	-0.762424	
H	2.886992	-0.473033	-0.67232	
O	1.759167	1.663196	0.213119	

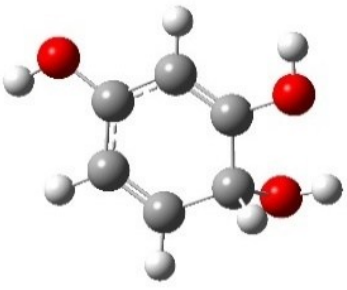

H	1.445905	2.562365	0.068491
H	1.791861	-0.693408	1.250115
O	-2.84099	0.539475	-0.256776
H	-3.438097	-0.21509	-0.237709

Water

Symbol	X	Y	Z	Internal Energy (Hartree)
O	0	0	0.117396	-76.4311385
H	0	0.75991	-0.469586	
H	0	-0.75991	-0.469586	

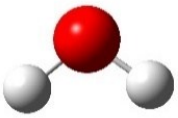

OH Radical

Symbol	X	Y	Z	Internal Energy (Hartree)
O	0	0	0.108045	-75.73318576
H	0	0	-0.864361	

H Radical

Atom	x	y	z	Internal Energy (Hartree)
H	0	0	0	-0.49815768

Atom Coordinates for Optimized Transition State Geometries

CatecholRT1

Symbol	X	Y	Z	Internal Energy (Hartree)
C	1.954128	-0.327771	0.07002	-383.1800957
C	0.984641	-1.128633	0.630342	
C	-0.35214	-0.692202	0.696174	
C	-0.66848	0.60624	0.249341	
C	0.313909	1.417804	-0.310228	
C	1.611932	0.948994	-0.398589	
H	2.974987	-0.673229	-0.000713	
H	1.231414	-2.109435	1.011119	
H	0.042249	2.400432	-0.667991	
H	2.372855	1.580702	-0.835417	
O	-1.922114	1.090906	0.325463	
H	-2.526814	0.395438	0.606188	
O	-1.269361	-1.581223	-1.000061	
H	-0.549426	-1.371897	-1.612283	
H	-1.077402	-1.246064	1.273518	

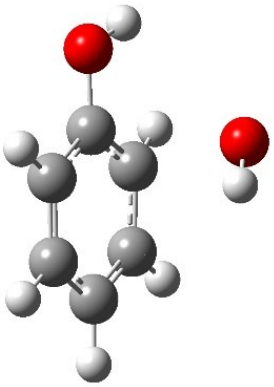

ResorcinolRT1

Symbol	X	Y	Z	Internal Energy (Hartree)
C	1.320037	0.92614	0.45497	-383.1745527
C	1.076271	-0.437076	0.736215	
C	-0.225724	-0.958287	0.57248	
C	-1.215142	-0.166738	0.032128	
C	-0.949211	1.168069	-0.306342	
C	0.311534	1.705785	-0.085342	
H	2.303524	1.336291	0.629375	
H	-1.745196	1.764714	-0.729578	
H	0.499736	2.740278	-0.334676	
O	-2.48113	-0.610755	-0.193275	
H	-2.56244	-1.530859	0.076109	
H	-0.431702	-1.986287	0.839977	
O	2.07067	-1.145974	-0.891113	
H	1.526296	-0.705223	-1.558787	
H	1.786868	-0.992443	1.328035	

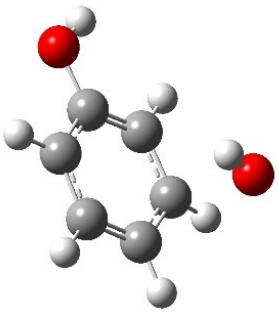

HydroquinoneRT1

Symbol	X	Y	Z	Internal Energy (Hartree)
C	1.309961	0.019225	0.052008	-383.1791487
C	0.63692	1.231134	-0.139173	
C	-0.6806	1.220073	-0.535604	
C	-1.371302	0.003355	-0.710056	
C	-0.659594	-1.203129	-0.564728	
C	0.660109	-1.199659	-0.168164	
H	1.169529	2.156793	0.025182	
H	-1.203107	2.153491	-0.689137	
H	-1.164271	-2.14248	-0.73996	
H	1.198913	-2.127738	-0.029883	

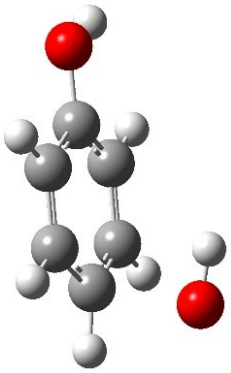

O	-2.399903	-0.042262	1.151151
H	-1.58599	-0.019483	1.673781
O	2.599305	0.086249	0.444968
H	2.967591	-0.797961	0.545002
H	-2.350842	-0.000507	-1.159633

Table S1 Conversion and selectivity on Au/ZnO catalysts with different lengths, where ZnO+LAuNRs = gold nanorods length ~300 nm width 20 nm; ZnO+SAuNRs = gold nanorods length ~ 55 nm width 20 nm

Conversion, %

	Reaction time (Hours)	ZnO+LAuNRs	ZnO+SAuNRs
UV	1	4	10
	2	7	17
	3	24	38
Vis	1	0	0
	2	0	0
	3	2	3

Selectivity, %

	Reaction time (Hours)	ZnO+LAuNRs	ZnO+SAuNRs
UV	1	HQ 100%	HQ 100%
	2	HQ 100%	HQ 100%
	3	HQ 100%	HQ 100%
Vis	1	-	-
	2	-	-
	3	HQ 100%	HQ 100%

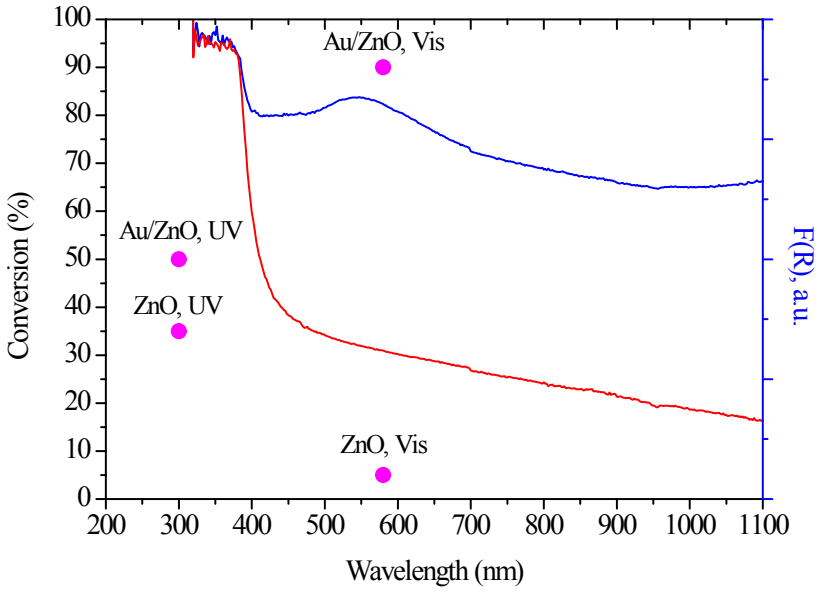

Fig. S18 The figure shows the conversion of phenol as a function of the main wavelength of the irradiation source vs. the absorption spectra of the catalysts. From this, it can be clearly deduced that the surface plasmon is responsible for the absorption and, thus, better activity of the Au/ZnO catalyst.